

Eagle Ford Condensed Section and Its Oil and Gas Storage and Flow Potential*

Roger M. Slatt¹, Neal R. O'Brien², Andrea Miceli Romero¹, and
Heidyli H. Rodriguez¹

Search and Discovery Article #80245 (2012)**

Posted July 31, 2012

*Adapted from an oral presentation at AAPG Annual Convention and Exhibition, Long Beach, California, April 22-25, 2012

**AAPG©2012 Serial rights given by author. For all other rights contact author directly.

¹University of Oklahoma, Norman, OK (rslatt@ou.edu)

²State University of New York at Potsdam, Potsdam, NY

Abstract

The Cretaceous Eagle Ford Shale in southwest Texas is actively being pursued for oil and gas. Results are presented of a scanning electron microscopy (SEM) study coupled with energy dispersive analysis (EDX) in evaluating the storage and flow potential for oil (and gas) in this shale.

The Eagle Ford Shale is calcareous (64% average CaCO₃); thus its properties and production performance cannot be directly compared to other common, more siliceous resource shales. However, it is like many other shales in containing an organic-rich condensed section (CS) immediately above a combined sequence boundary (SB) and transgressive surface of erosion (TSE); in this case the upper surface of the Buda Limestone. An excellent exposure of this CS occurs at “Comstock West” a roadcut located along Highway 90 about 30 miles NW from Del Rio, Texas. Here, the shale weathers gray; but is black and has a strong hydrocarbon odor on a fresh surface. TOC averages 5.3%, and it contains Type II kerogen, making it an excellent marine oil and gas source rock. However, at this location the rocks are thermally immature with T_{max} values of 423-429°C and average R_o of 0.53%.

Scanning electron microscopy (SEM), coupled with energy dispersive X-ray analysis (EDX), has indicated „total area porosity“ can reach 10%, and „individual pore area“ can range up to 0.2µm². SEM/EDX analyses have also revealed the presence of at least three important pore types associated with: a) floccules, b) coccospheres, and c) foraminifera. Floccules are particularly well developed and provide pores up to 1µm in diameter. Both the internal chambers of coccospheres and their spines are hollow, open, and up to 1µm in diameter and several micrometers long. Nanopores also exist between the randomly oriented coccolith plates in the matrix. Hollow, internal chambers of foraminifera can be 10s of micrometers in diameter. Hydrous pyrolysis treatment followed by SEM/EDX has produced oil within some of the pores, thus providing clues as to residual oil generation and primary migration. Results indicate that the calcareous condensed section within the Eagle Ford has ample storage and flow potential for oil (and gas) relative to some of their more siliceous counterparts.

References

Donovan A.D., T.S. Staerker, L. Weiguo, A. Pramudito., J. Evenick, T. McClain, A. Agrawal, L. Banfield,, S. Land, M.J. Corbett., C. M. Lowery, and A. Miceli Romero, (eds.), 2011, Field guide to the Eagle Ford (Boquillas) Formation: West Texas: AAPG Field Seminar Guide Book, Terrell County, TX, April 2011.

O'Brien, N.R., and R.M. Slatt, 1990, The fabrics of shales and mudstone; an overview, *in* J.F. Burst, W.D. Johns, (chairs) Clay Minerals Society, 27th annual meeting, program and abstracts: Clay Minerals Annual Conference, v. 27, p. 99.

Pollastro, R.M., 2007, Total petroleum system assessment of undiscovered resources in the giant Barnett Shale continuous (unconventional) gas accumulation, Fort Worth Basin, Texas, *in* R.J. Hill, and D.M. Jarvie, (eds.), Special Issue; Barnett Shale: AAPG Bulletin, v. 91/4, p. 551-578.

Schieber, J., J. Southard, and K. Thaisen, 2007, Accretion of mudstone beds from migrating floccule ripples: *Science*, v. 318/5857, p. 1760-1763.

Singh, P., 2008, Lithofacies and sequence stratigraphic framework of the Barnett Shale, northeast Texas: Ph.D., University of Oklahoma, Norman, Oklahoma, 181 p.

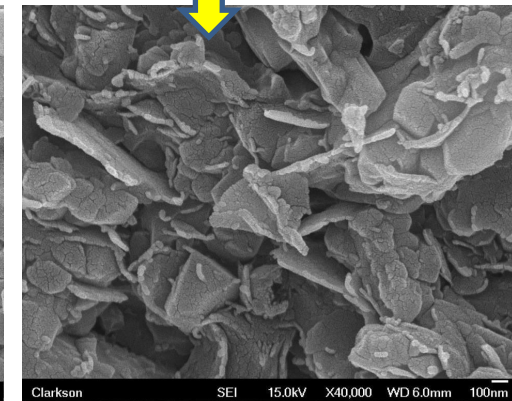
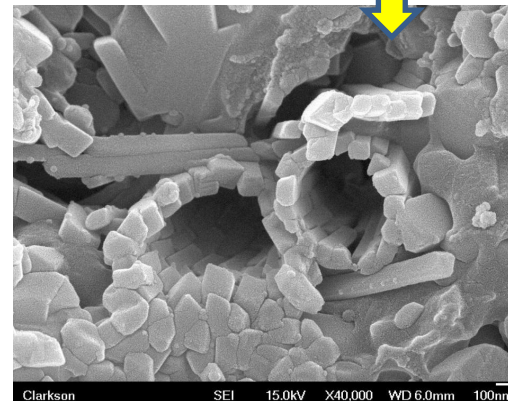
Slatt, R.M., and N.D. Rodriguez, 2012, Comparative sequence stratigraphy and organic geochemistry of gas shales: Commonality or coincidence: *Journal of Natural Gas Science and Engineering*, v. 8, p. 68-84.

Slatt, R.M., and N.R. O'Brien, 2011, Pore types in the Barnett and Woodford gas shales; contribution to understanding as storage and migration pathways in fine-grained rocks: *AAPG Bulletin*, v. 95/12, p. 2017-2030.

Comstock West outcrop

Calcareous mudstone and wackestone

Calcareous mudstone



Clarkson SEI 15.0kV X40,000 WD 6.0mm 100nm

Clarkson SEI 15.0kV X40,000 WD 6.0mm 100nm

Eagle Ford Condensed Section and its Oil and gas storage and flow potential

Roger M. Slatt¹

Neal R. O'Brien²

Andrea Miceli Romero¹

Heidyli H. Rodriguez¹

¹ University of Oklahoma

² State University N.Y. at Potsdam

Sponsors of Shale Pore Consortium



Lozier Canyon, South Texas Outcrop

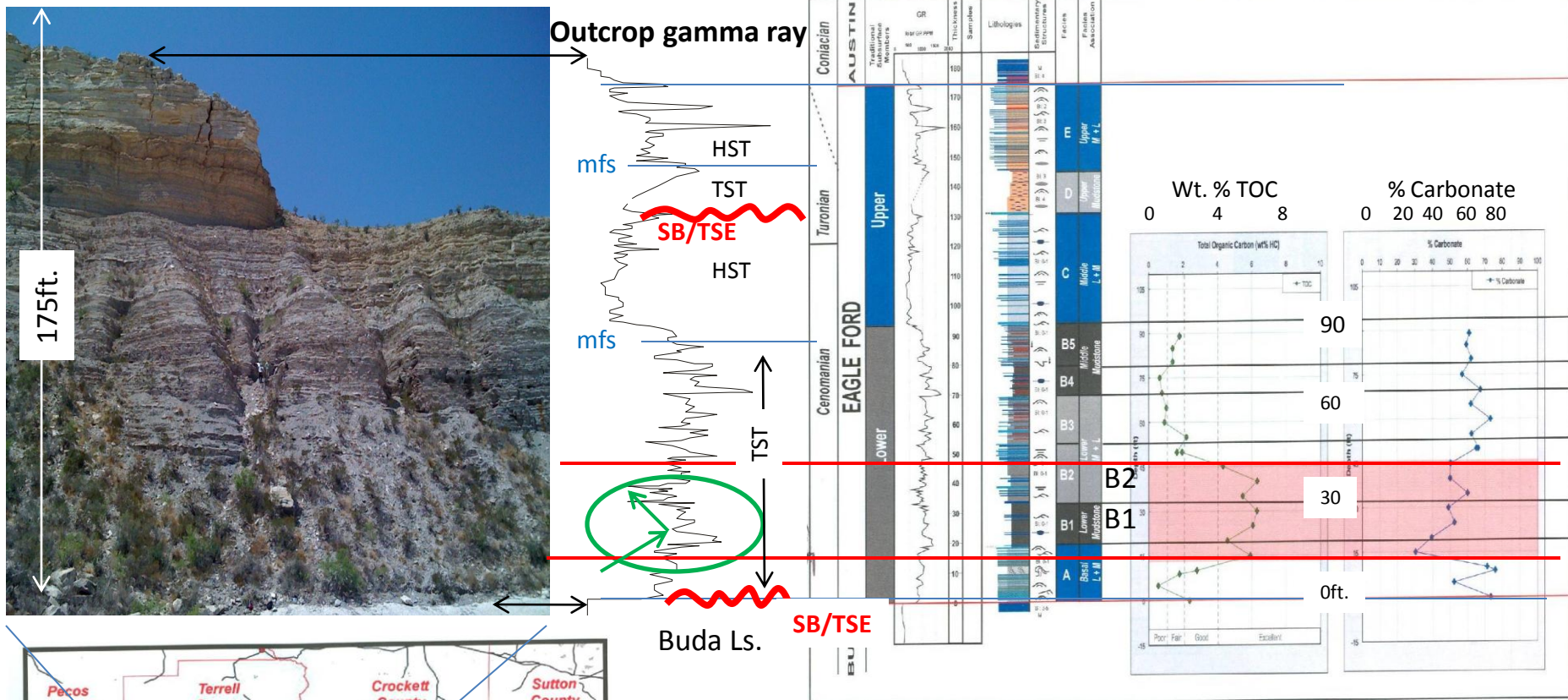


Figure S2.28: TOC values of 4-6% occur in Facies B1, as well as the basal portions of B2 on top of A. The higher TOC values coincide with intervals of lower carbonate content. Section legend on Figure S2.11. Geochemical data from Andrea Miceli Romero.

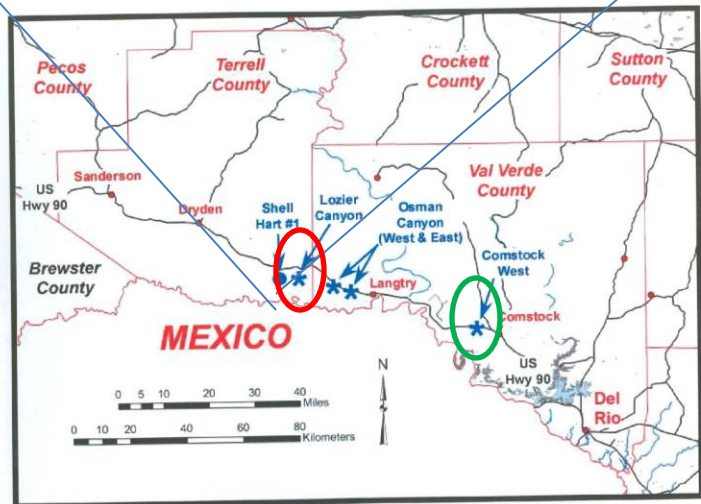
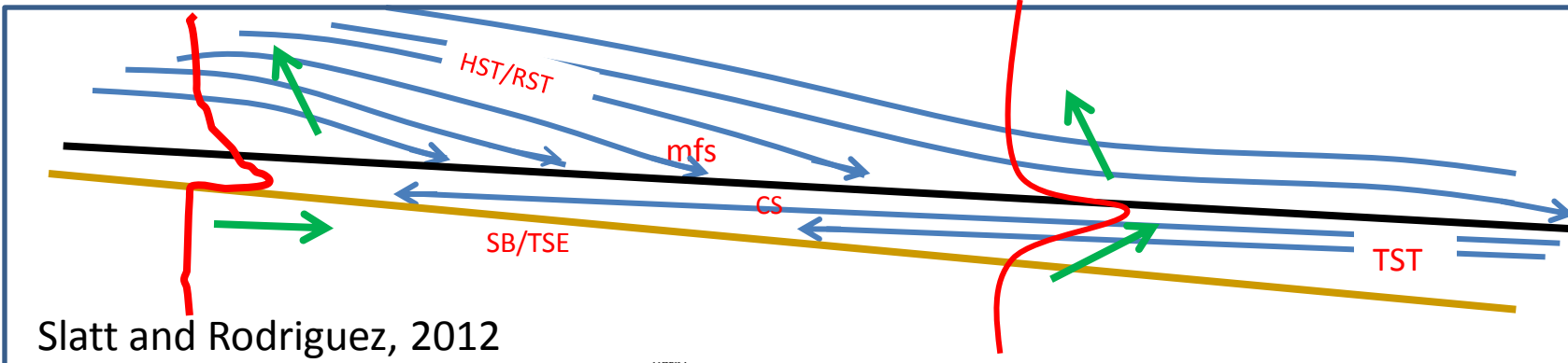


Figure O8: Location map illustrating the key outcrop localities along U.S. 90, northwest of Del Rio in Val Verde and Terrell Counties, Texas, along with the position of the Shell Hart 1 well.

Figures From: Donovan A. D., Staerker T. S., Weiguo L., Pramudito A., Evenick J., McClain T., Agrawal A., Banfield L., Land S., Corbett M. J., Lowery C. M., and Miceli Romero A. "Field guide to the Eagle Ford (Boquillas) Formation: West Texas". AAPG Field Seminar Guide Book, Terrell County, TX, April 2011.

Landward

Seaward



Slatt and Rodriguez, 2012

Singh, 2008

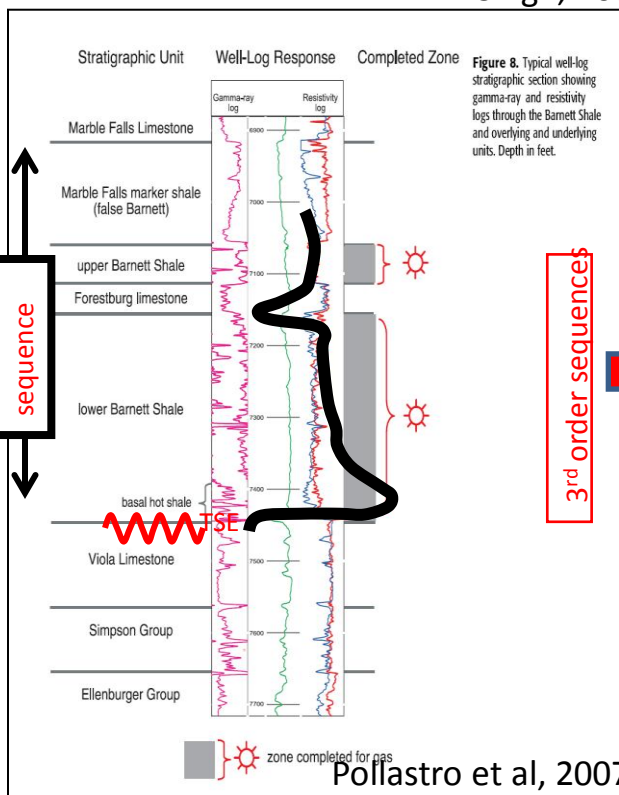
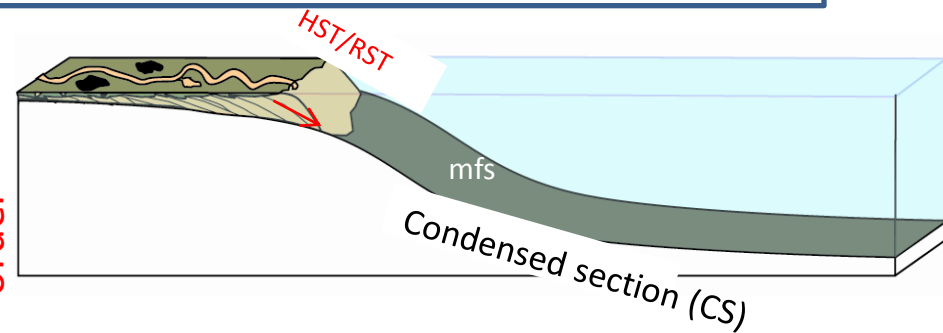
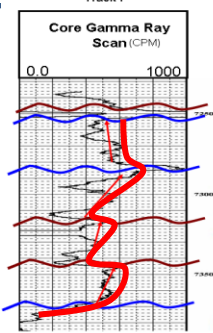
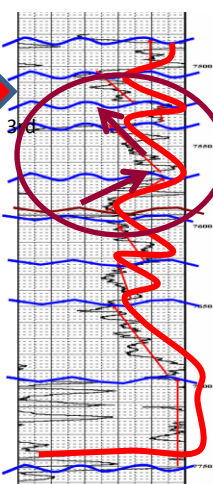


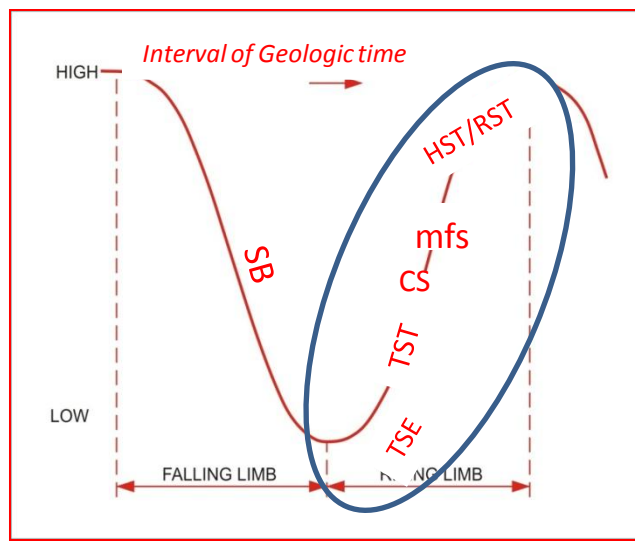
Figure 8. Typical well-log stratigraphic section showing gamma-ray and resistivity logs through the Barnett Shale and overlying and underlying units. Depth in feet.



3rd order sequences



22/15 = 1.5my = 3rd order



Typical Well Log Patterns of Barnett Shale

Pollastro et al, 2007

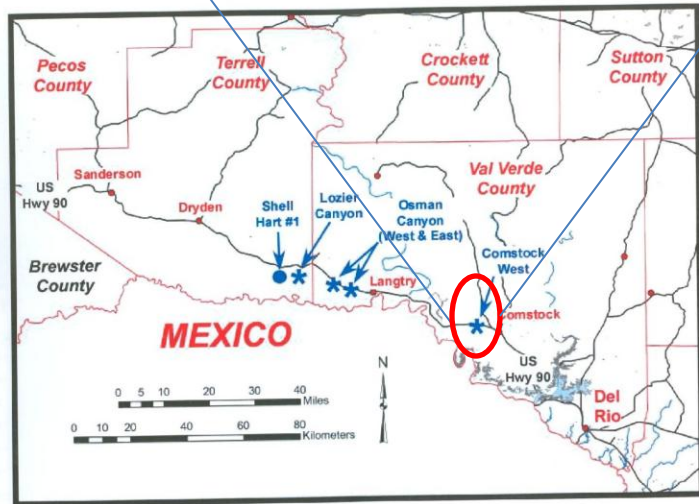
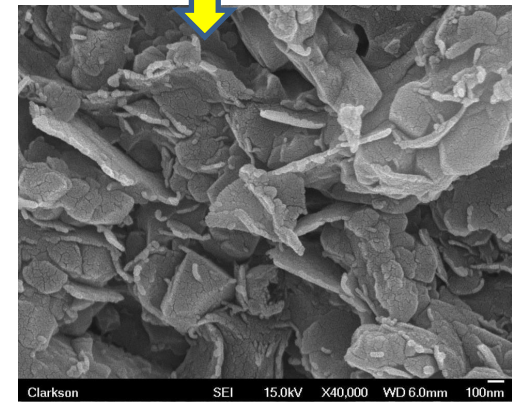
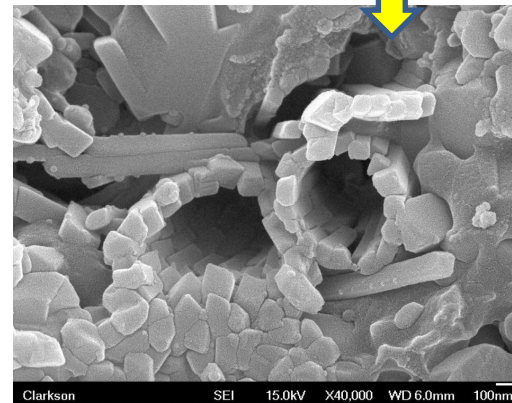
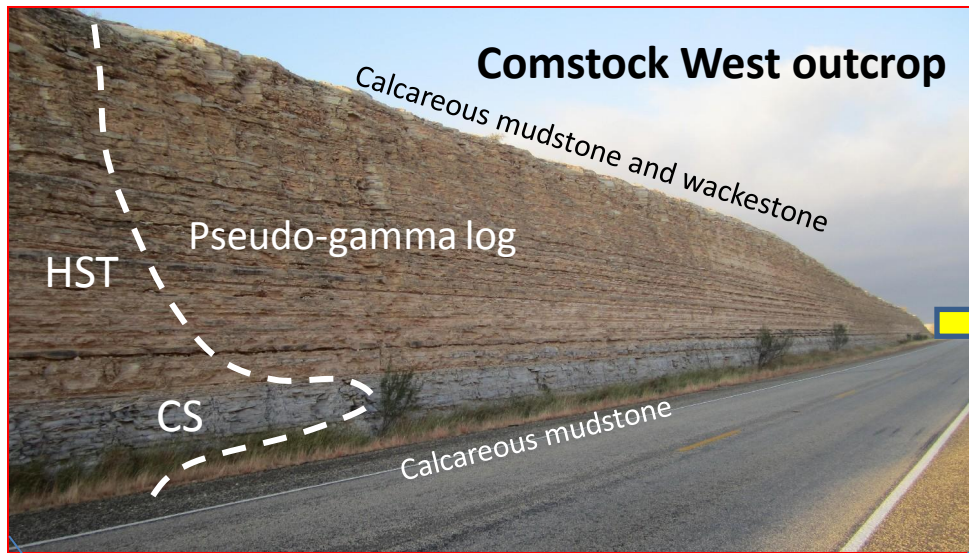
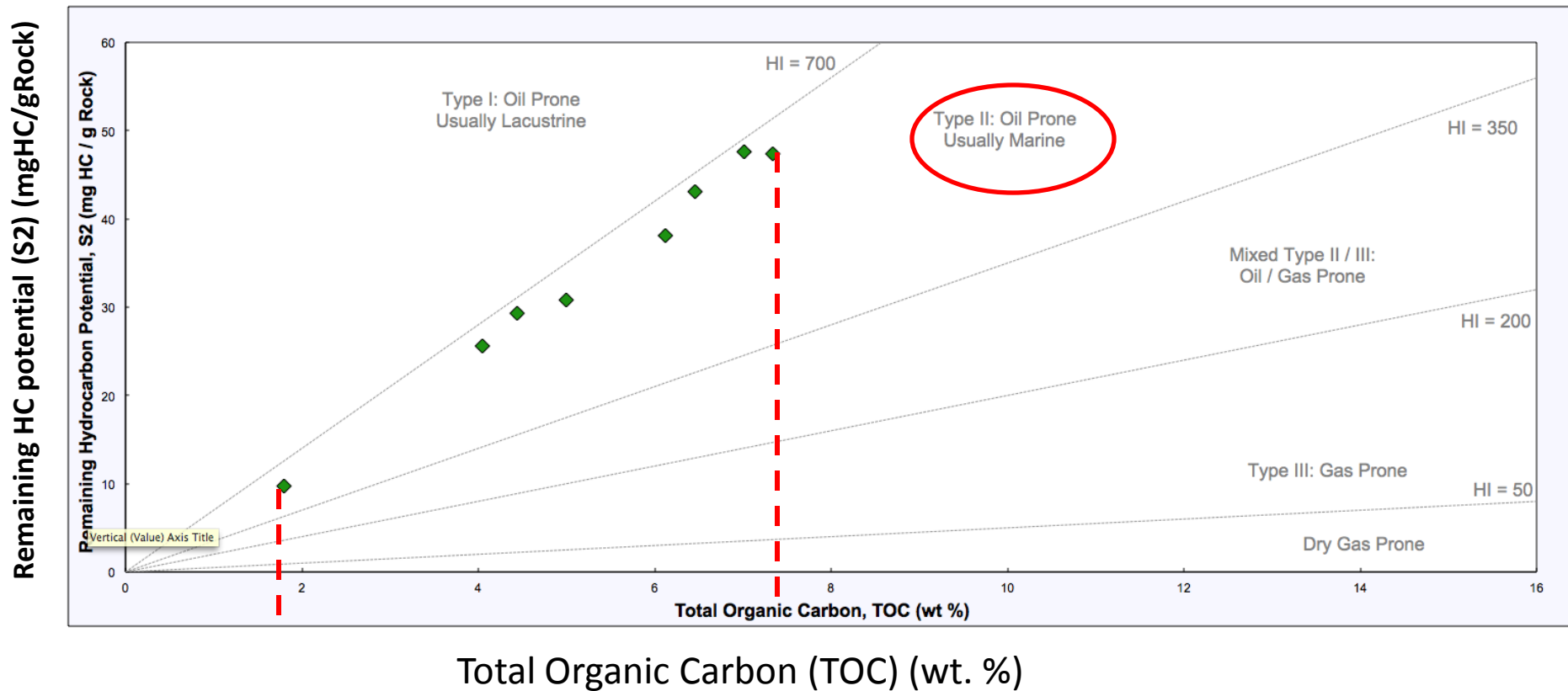


Figure O8: Location map illustrating the key outcrop localities along U.S. 90, northwest of Del Rio in Val Verde and Terrell Counties, Texas, along with the position of the Shell Hart 1 well.

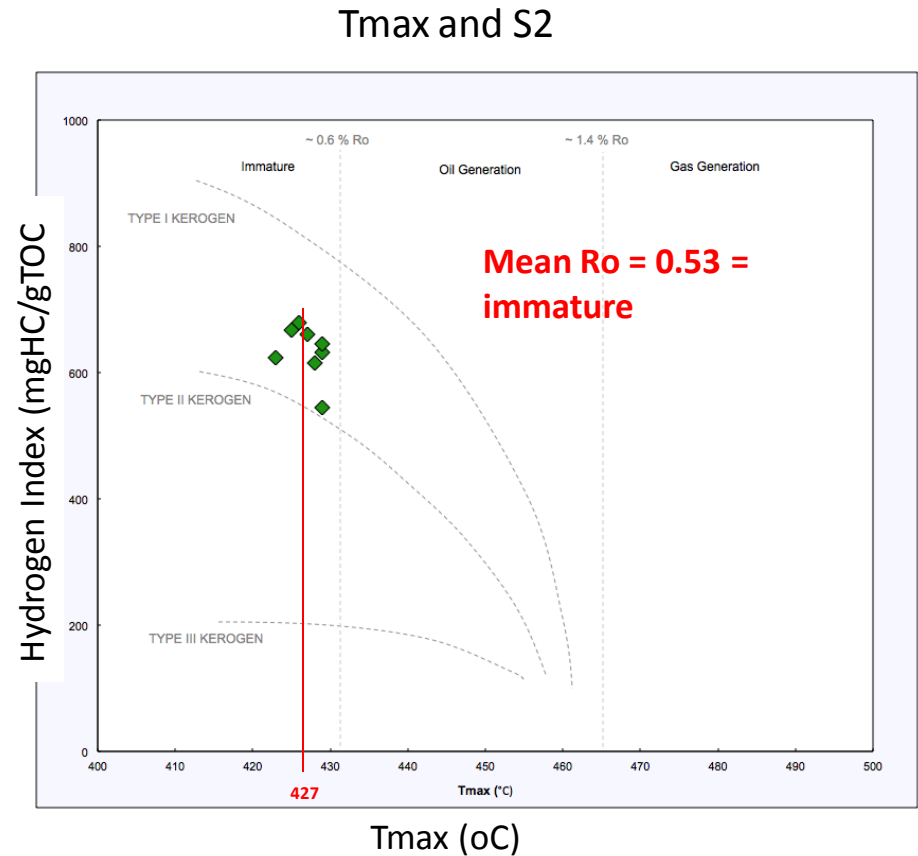
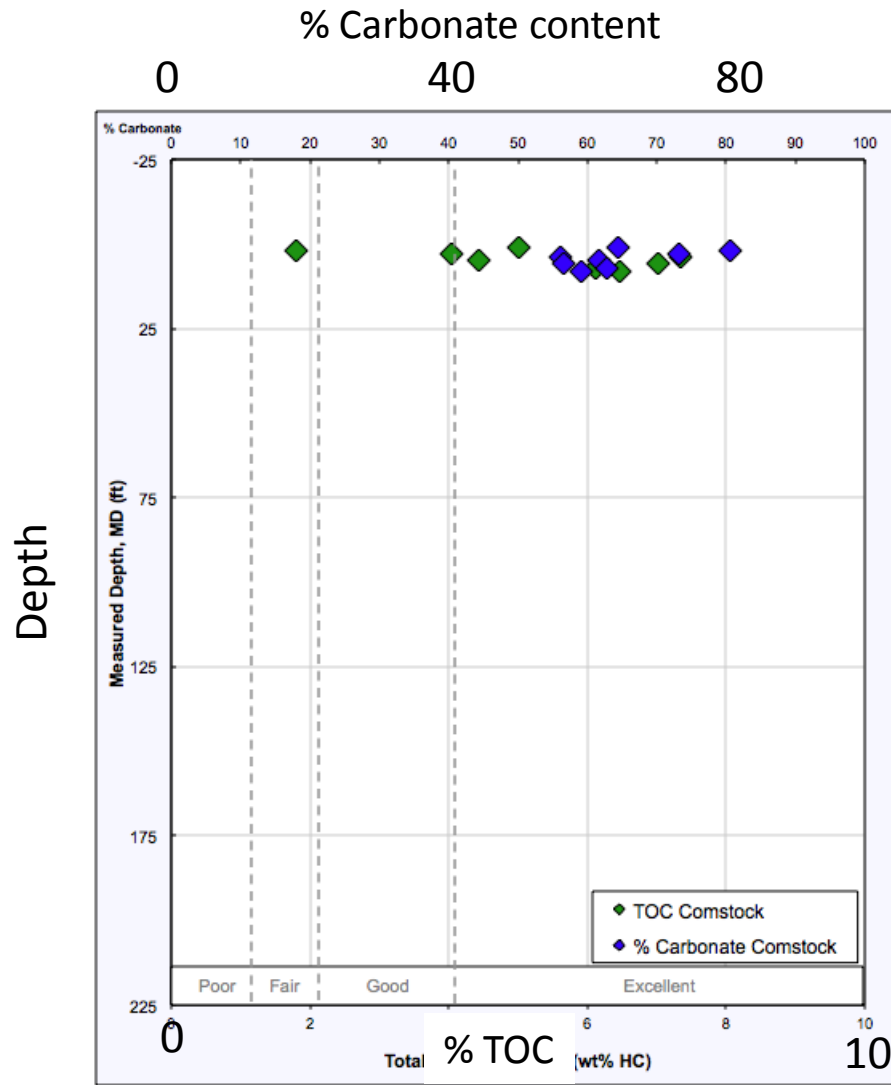
Source-Rock Analysis

Kerogen Quality



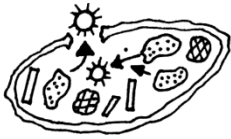
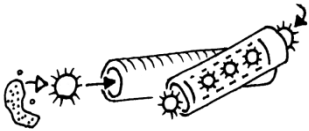
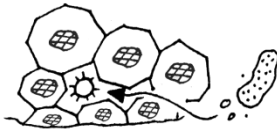
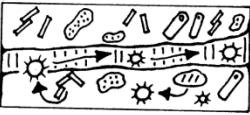


A plot between S2 and TOC shows the Type II kerogen quality of the Eagle Ford Shale samples

Source-Rock Analysis










Eagle Ford Shale samples collected at the Comstock West outcrop are organic rich, with an **average TOC value of 5.28%**, meaning that these rocks **have excellent source quality, also indicated by its high S2 values**. In this outcrop, samples have a thin, weathered, white layer; however, a fresh sample is dark gray and emanates a strong hydrocarbon smell. In addition, these samples are carbonate-rich, with an **average carbonate content of 64.31%**.

Pore Type	Image	Distinctive Features
Porous Floccules		Clumps of electrostatically charged clay flakes arranged in edge-face or edge-edge cardhouse structure . Pores up to 10s of microns in diameter. Pores may be connected.
Organo-porosity		Pores in smooth surfaces of organic flakes or kerogen . Pore diameters are at nanometer scale . Pores are generally isolated. Porous organic coatings can also be adsorbed on clays.
Fecal Pellets		Spheres/ellipsoids with randomly oriented internal particles, giving rise to intrapellet pores . Pellets are sand-size and may be aligned into laminae.
Fossil Fragments		Porous fossil particles , including sponge spicules, radiolaria, and cysts (<i>Tasmanites?</i>). Interior chamber may be open or filled with detrital or authigenic minerals.
Intraparticle Grains/Pores		Porous grains , such as pyrite framboids which have internal pores between micro-crystals. Grains are of secondary origin, and are usually dispersed within the shale matrix.
Microchannels and Microfractures		Linear nano-micrometer-sized openings that often cross-cuts bedding planes. Occur at nano-meter and larger scales.

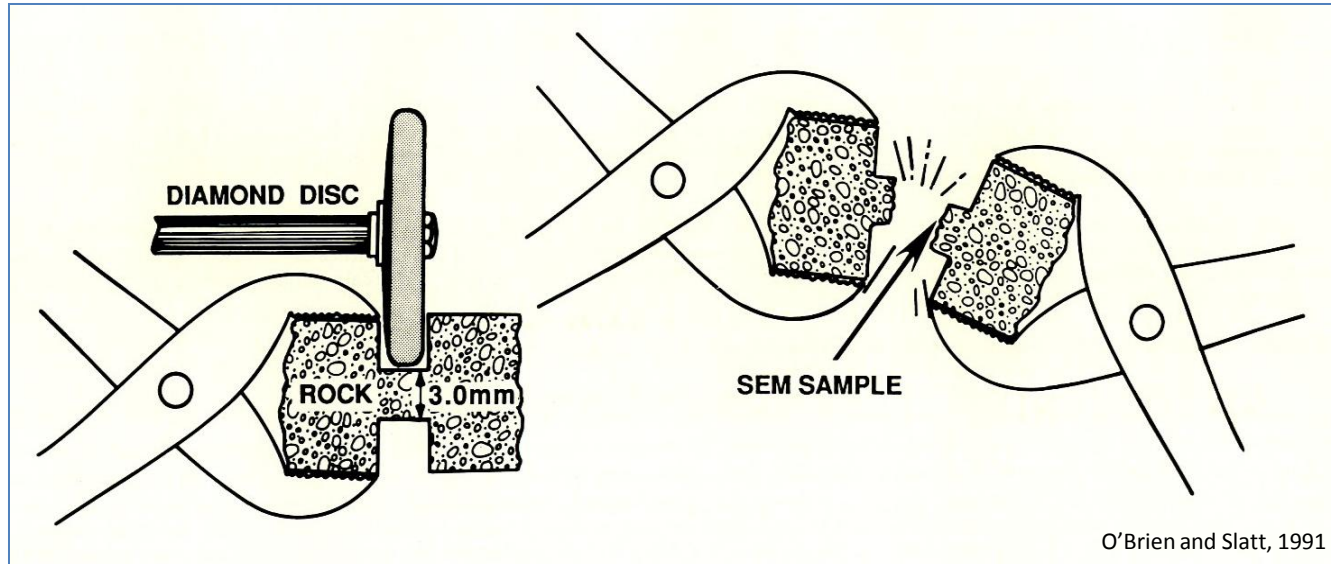
Classification of pore types in shales.

Slatt and O'Brien, 2011

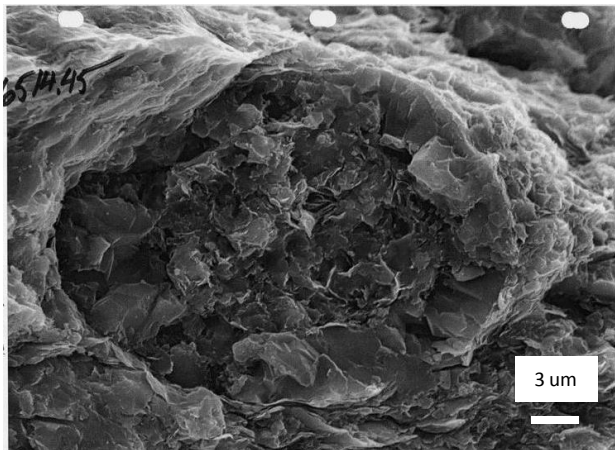
Symbols used:

	Clay Flake		Organic particle		Silt grain
	Fossil fragment		Gas		Gas migration
	Microchannel microfracture				

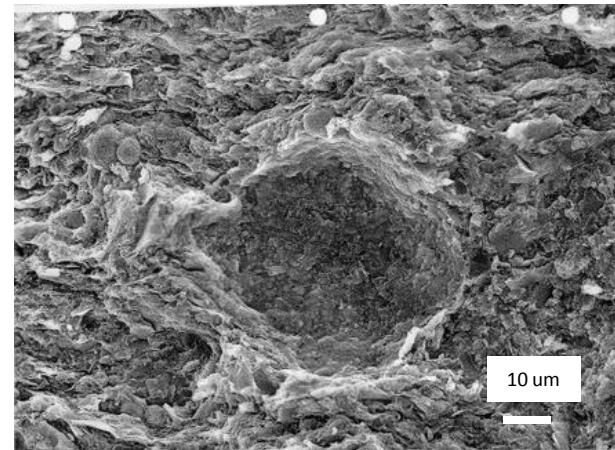
SEM SAMPLE PREPARATION



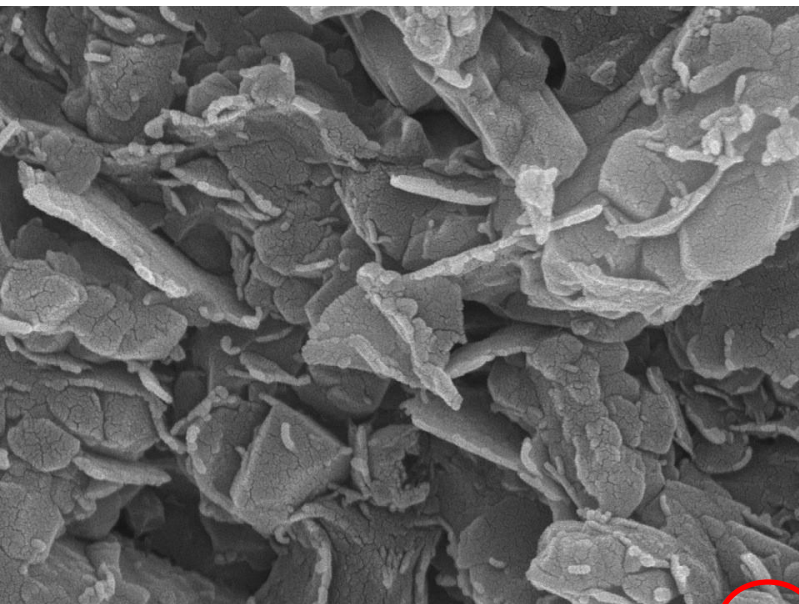
Care must be taken to ensure that 'pores' are not holes from plucked grains



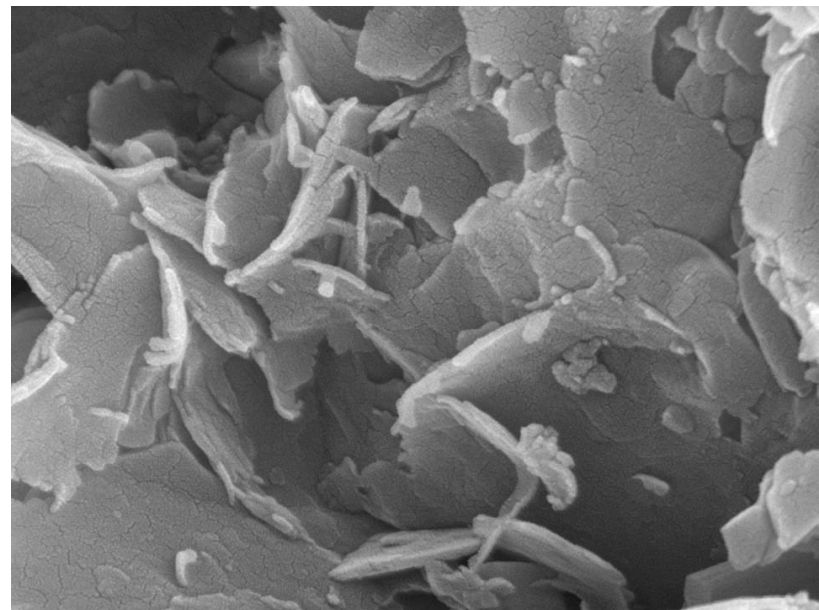
Fecal pellet with tangential clay flakes due to compaction.



Hole from plucked grain. Note tangential clay flakes, which are common for plucked holes (artificial pores).

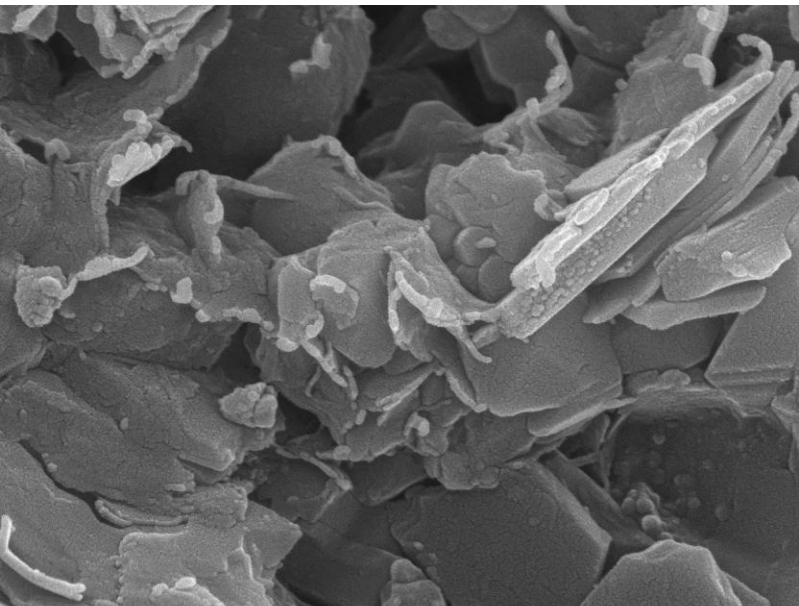


Clarkson SEI 15.0kV X40,000 WD 6.0mm 100nm

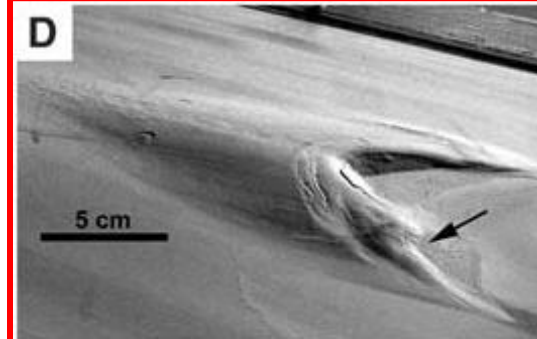
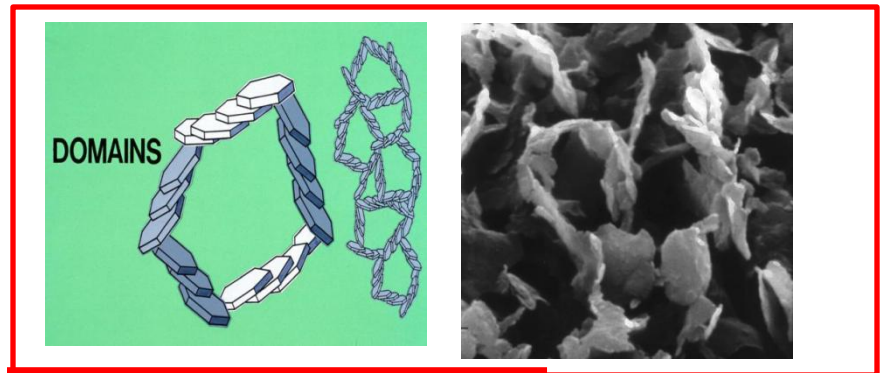


Clarkson SEI 15.0kV X60,000 WD 6.0mm 100nm

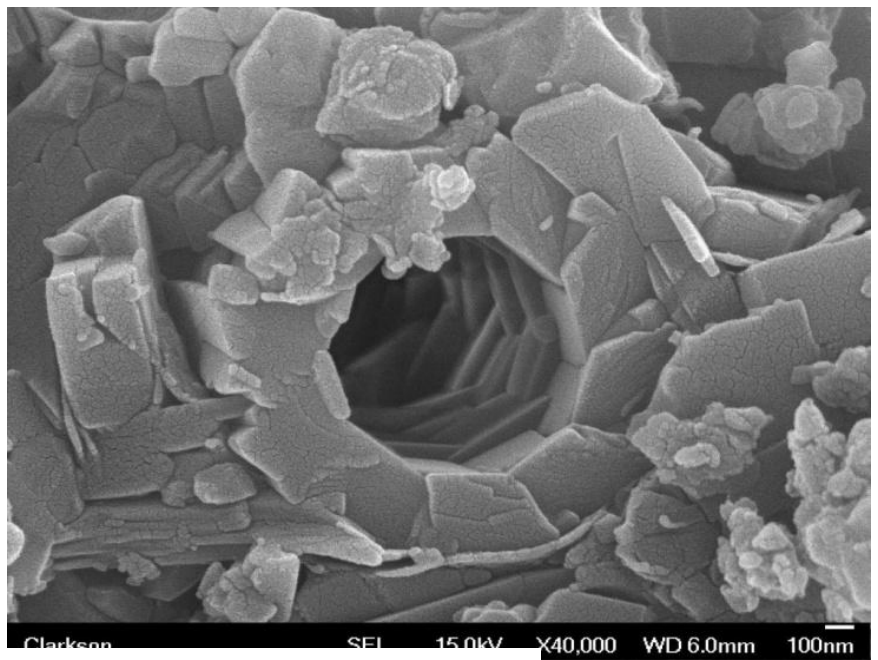
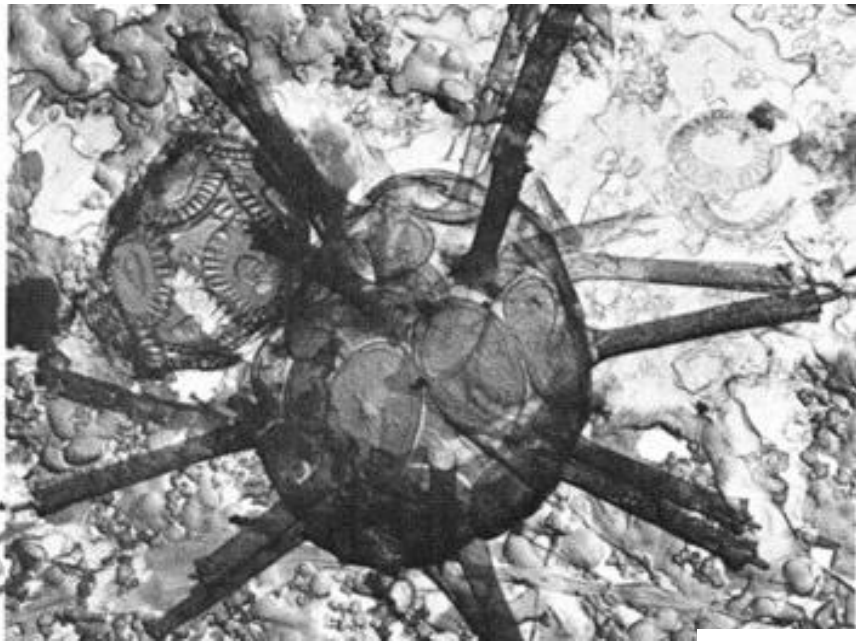
Floccules



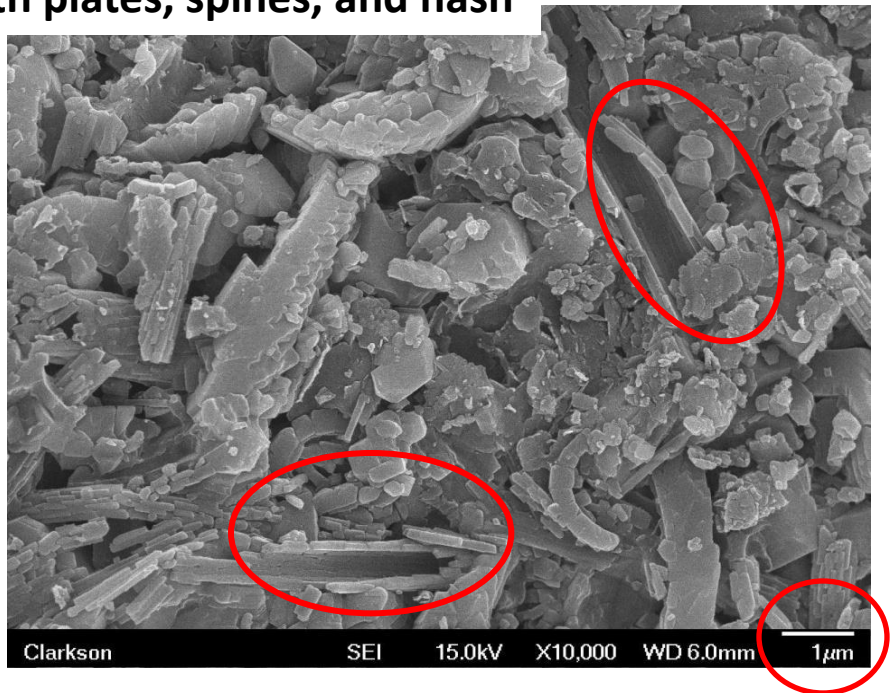
Clarkson SEI 15.0kV X40,000 WD 8.0mm 100nm

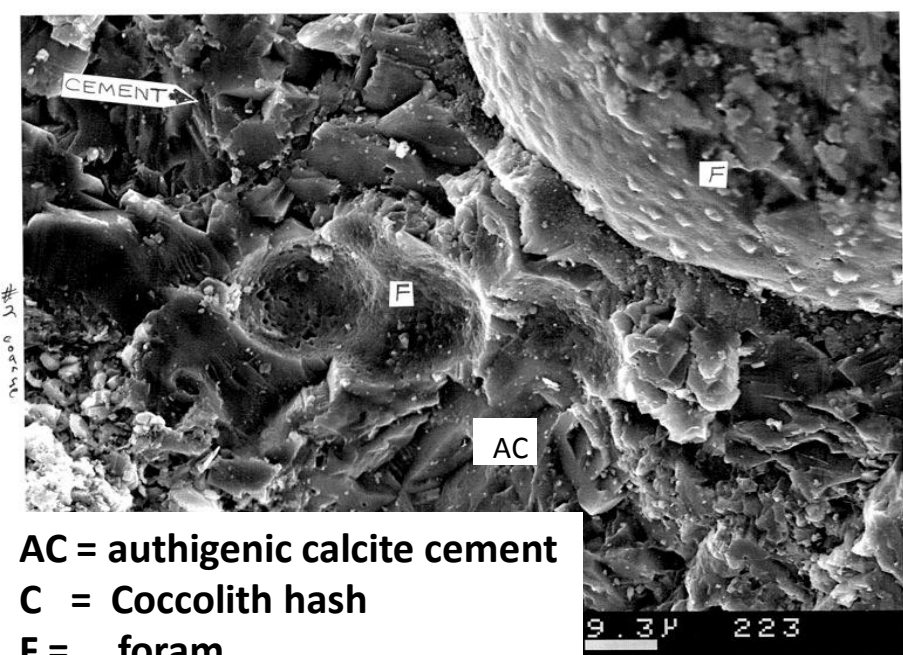


Schieber et al.
www.sciencemag.org
on December 14, 2007

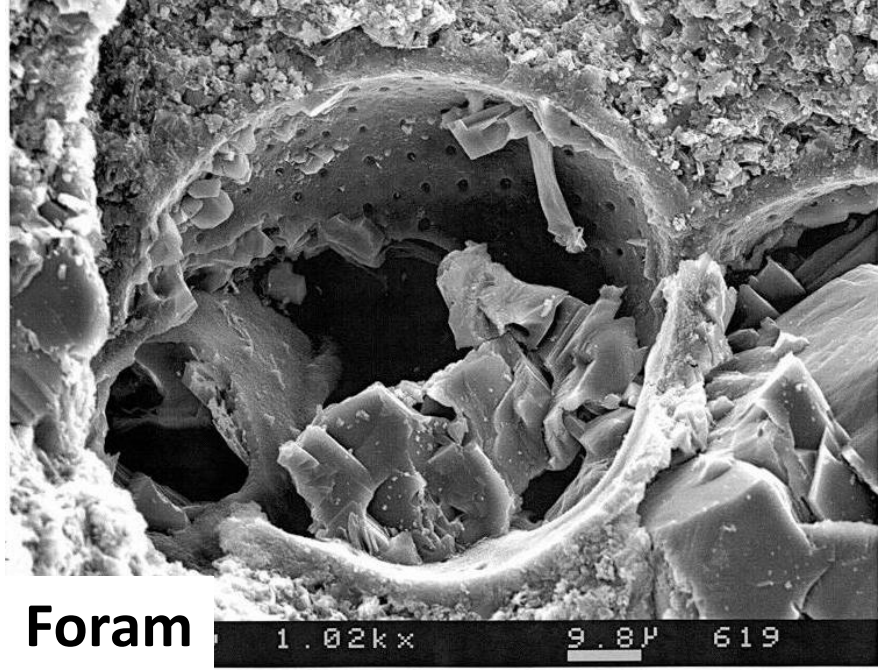


Coccolith plates, spines, and hash

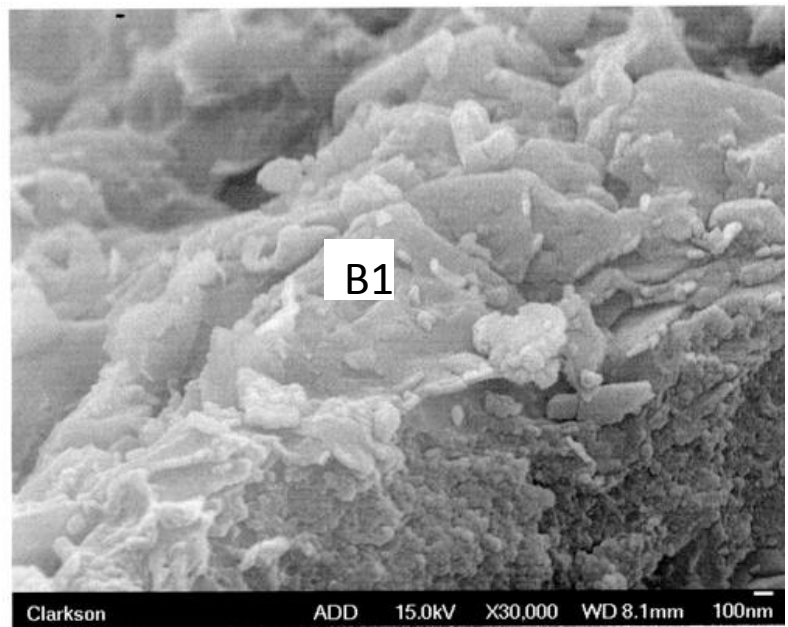




AC = authigenic calcite cement
 C = Coccolith hash
 F = foram

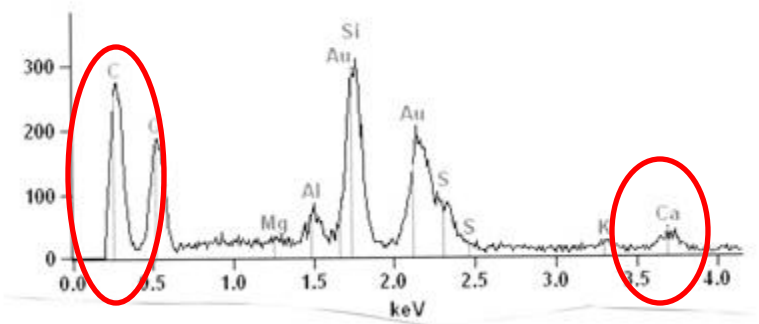


Foram



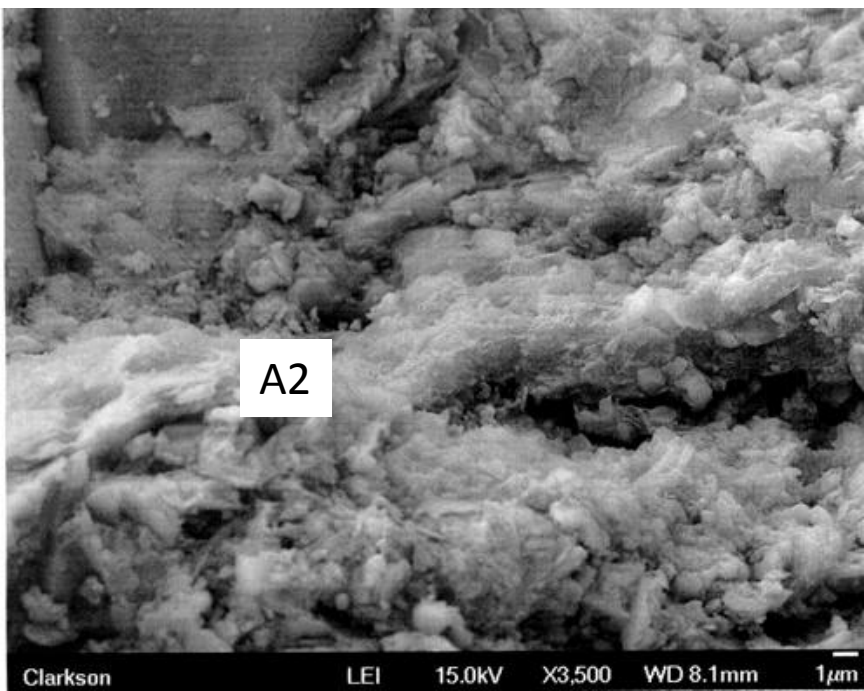
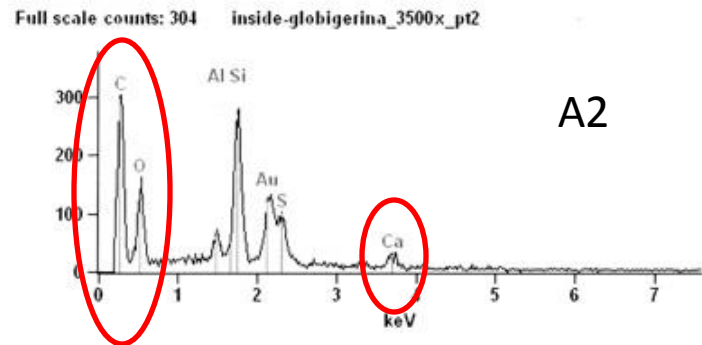
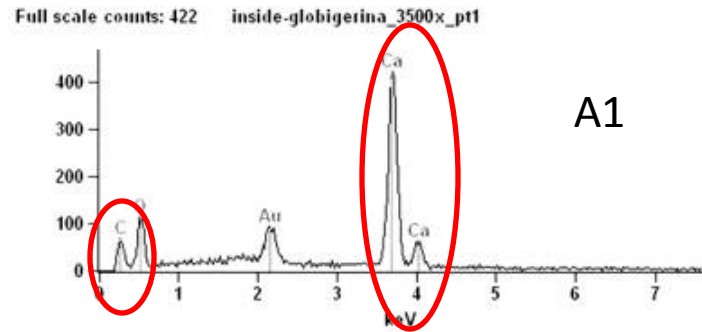
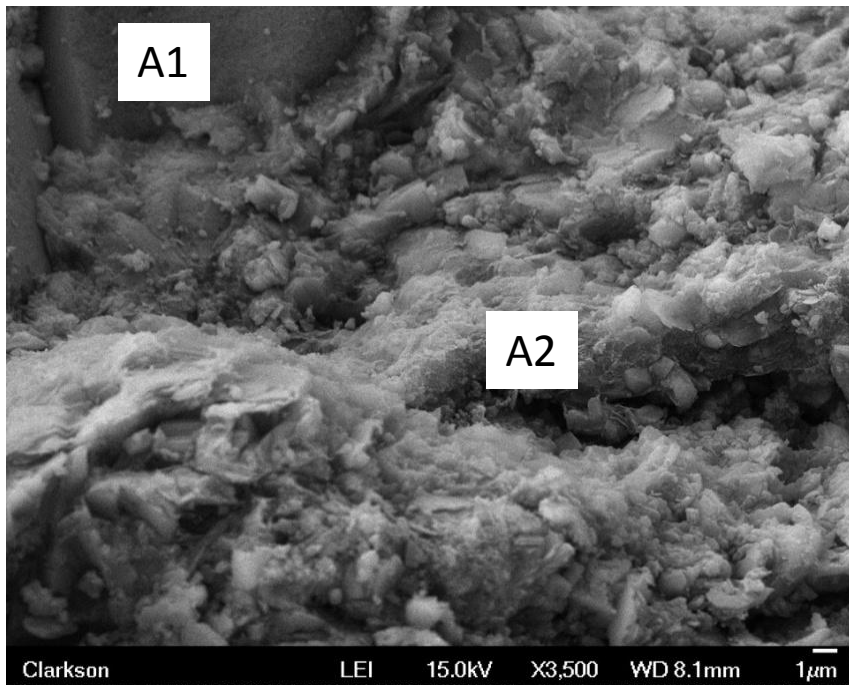
B1 = organic-clad clay particle

“Organic-clad clay flakes”

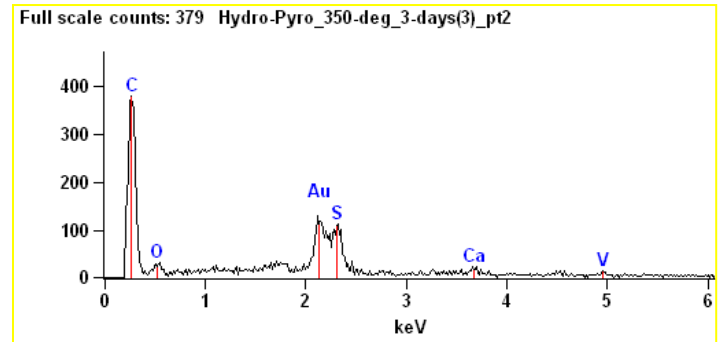
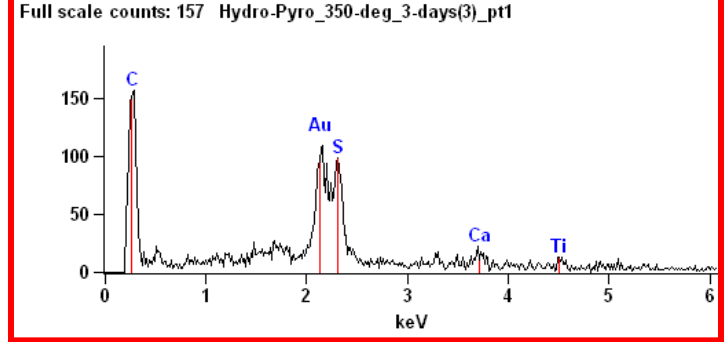


	Weight %							
	C	O	Mg	Al	Si	S	K	Ca
<i>inside-globigerina 250k pt1</i>	62.16	26.82	0.17	0.92	6.41	1.71	0.43	1.39

EDAX analysis



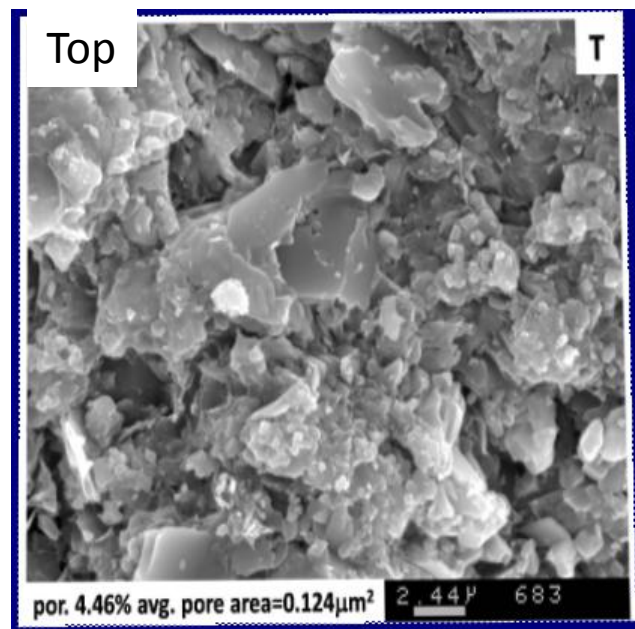
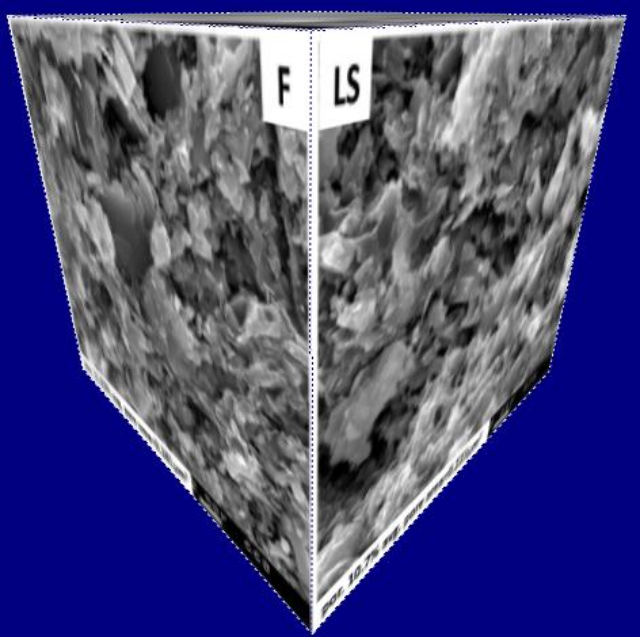
		Weight %							
		C	O	Al	Si	S	K	Ca	Ba
A1	inside-globigerina_3500x_pt1	20.36	39.39					40.25	
	inside-globigerina_3500x_pt2	69.48	20.23	0.91	5.70	2.24		1.45	
A2	inside-globigerina_3500x_pt3	23.26	48.68	1.23	3.33	9.99	0.70		
	inside-globigerina_3500x_pt4	28.97	40.99	0.55	3.30	4.59		12.81	5.58
	inside-globigerina_3500x_pt5	27.57	41.60	0.52			0.53	16.03	
	inside-globigerina_3500x_pt6	55.99	31.35	1.02	12.46	5.35		17.32	
	inside-globigerina_3500x_pt7	55.99	31.35	1.15	5.35			6.29	
	inside-globigerina_3500x_pt8	47.88	35.04	1.15	12.27	1.86		1.80	
	inside-globigerina_3500x_pt9	47.88	35.04	1.15	12.27	1.86		1.80	



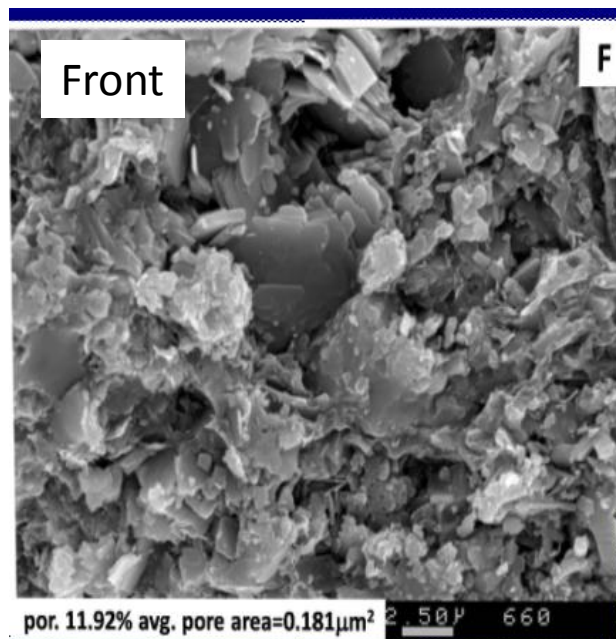
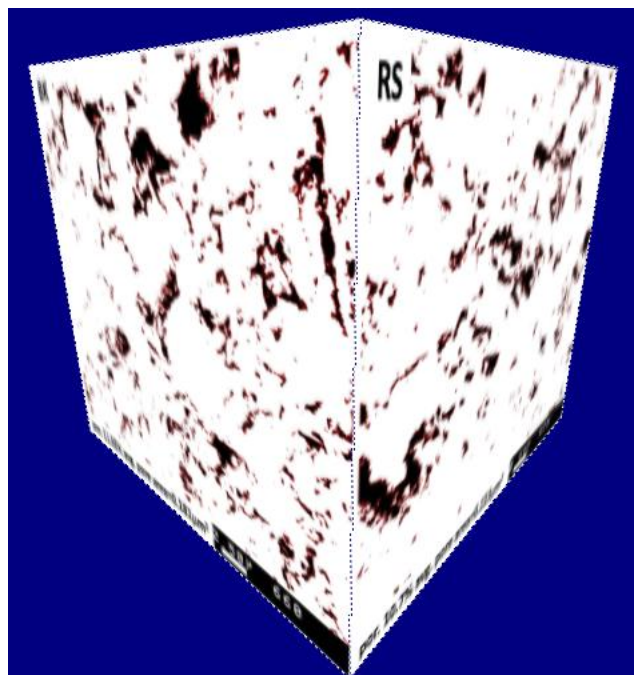
Post-Hydrous Pyrolysis

Furnace and sample holder (arrow) used in hydrous pyrolysis experiments. 350oC for 4 days.

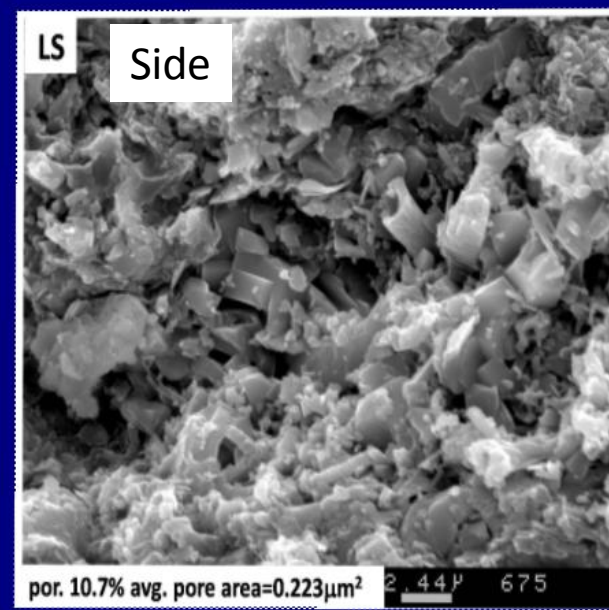




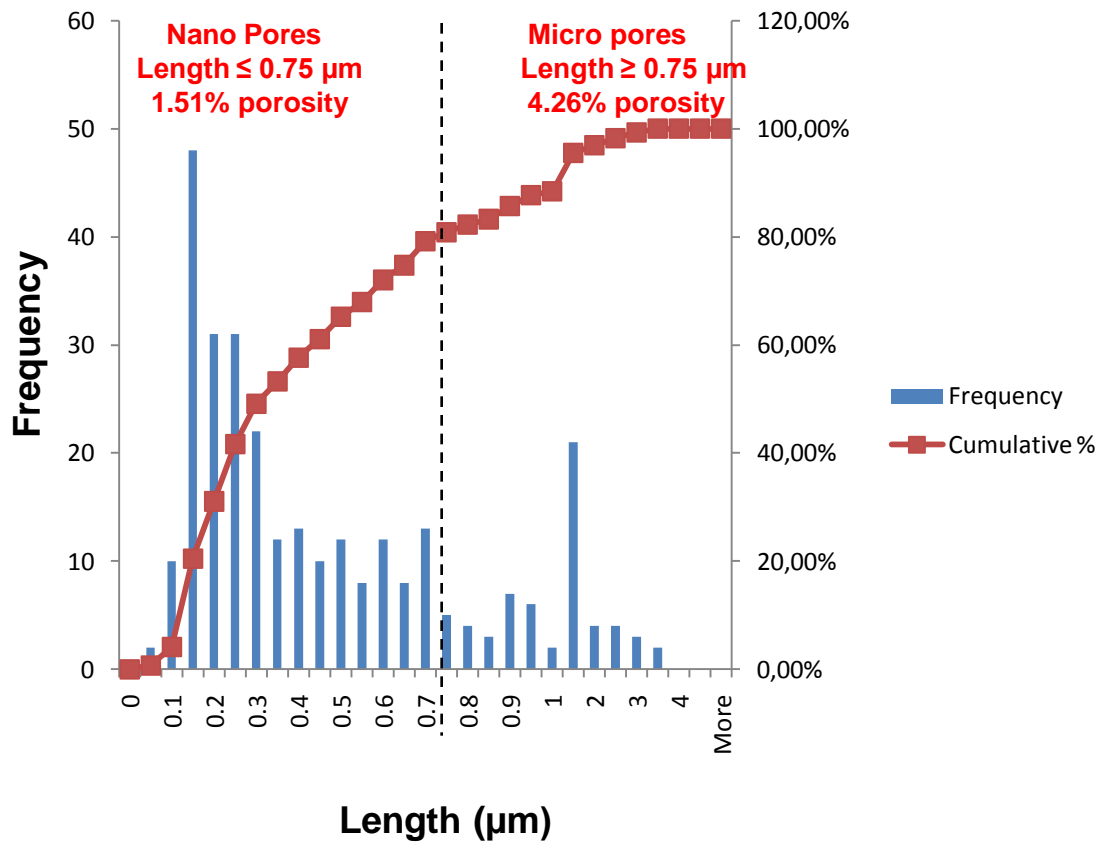
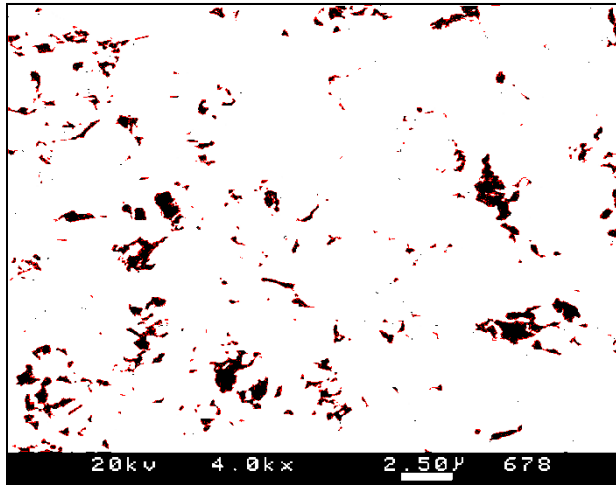
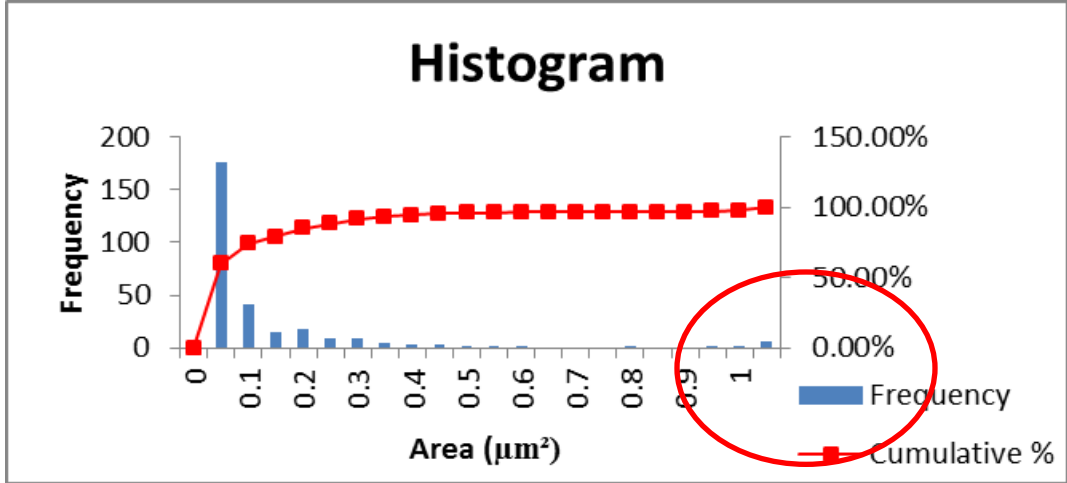
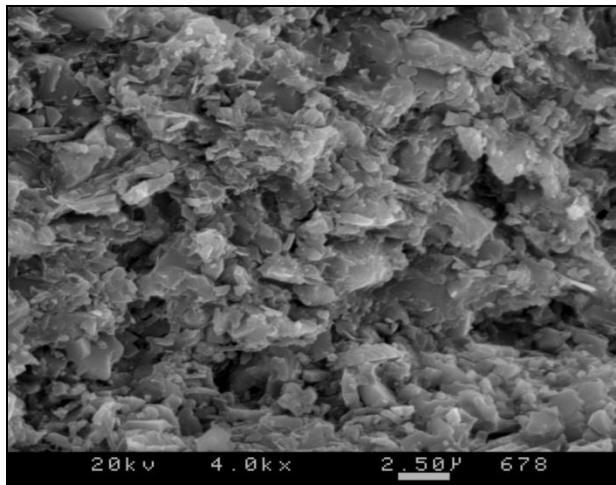
4.5% por.



11.9% por.



10.7% por.



Porosity calculated: 5.8%
 Number of pores: 293
 Average area: 0.123µm²

Conclusions:

- Comstock West outcrop is a high-frequency stratigraphic sequence.
- Condensed section is a good, thermally mature, Type II source rock.
- Several different pore types observable under an SEM/FESEM
- Abundance, size and types of pores can be identified and measured.
- Micropores ($>0.75\mu\text{m}$) contribute more to porosity than nanopores ($<0.75\mu\text{m}$). Viewing small SEM images (few μm) can be misleading.
- These pore types can store and transfer free gas and liquids. All pores must be included in calculating free gas/oil in shale.